Nonlinear Dynamics and Systems Theory, **21** (2) (2021) 202–215

Dynamics of Nonlinear Longitudinal Vibrations in a 1D Nano-Scale Continuum Described by the Generalized Morse Potential

S. A. Surulere *, M. Y. Shatalov, A. C. Mkolesia and I. Fedotov

Department of Mathematics and Statistics, Tshwane University of Technology, P.O. Box X680, Pretoria, 0001*, South Africa.*

Received: October 3, 2020; Revised: January 21, 2021

Abstract: A continuum which was described by a governing second-order partial differential equation (PDE), containing an infinite attachment of atoms, was detailed. We formulated the governing PDE using Hamilton's principle and derived the boundary conditions. Four different boundary conditions were formulated but we assumed that the left end of the continuum was fixed, $u(t, r = 0) = 0$, while the right end was free, $\left.\frac{\partial u}{\partial r}\right|_{r=l} = 0$. The method of lines was employed and used to convert the governing PDE into a coupled system of infinite ordinary differential equations (ODEs). The system of coupled ODEs was numerically integrated within the time interval, $t \in [0, 4\pi]$. It was observed that the trough of the waves became sharply triangular for lower grid points and smooth for higher grid points.

Keywords: *generalized Morse potential; Hamilton's principle; method of lines; nonlinear interactions; periodic motion.*

Mathematics Subject Classification (2010): 70K25, 70H03, 70H25, 35L05.

* Corresponding author: mailto:samuel.abayomi.sas@gmail.com

© 2021 InforMath Publishing Group/1562-8353 (print)/1813-7385 (online)/http://e-ndst.kiev.ua

1 Introduction

The analysis of vibrations in a mechanical system is very crucial to engineers because neglecting the vibrations in a system can result into wears, tears, and an eventual system breakdown. It can be observed that from a cell to a community of organisms, from an atom to galaxies, oscillatory processes are a fundamental characteristic of all organic and inorganic nature [1]. This makes the philosophic significance of the science of vibrations absolutely necessary [1]. The bodies in the nano-scale dimensions are not exempted from these studies. Morikazu Toda studied and proposed the well-known Toda lattice. His proposed lattice is one-dimensional and has nonlinear interactions that were described by a potential having one exponent [2]. His results and subsequent findings were later published as a book [3].

In this paper, we will construct a nanochain, described as a continuum containing an attachment of infinite atoms, using Hamilton's principle. The finite-difference scheme and Maclaurin series can also be used to formulate the governing PDE. The disadvantage of the former is that the Lagrangian formalism automatically conserves energy. The interaction potential between the atoms in the continuum is chosen as the Generalized Morse potential. The potential is one of the hybrid forms of the Morse potential [4].

The exact solution of the governing second-order PDE to be formulated, is very difficult to obtain. Hence, the method of lines (MOL) will be used to obtain a numerical solution of the governing PDE. The MOL details the conversion of a PDE into a coupled system of ODEs using the discretisation of the space variable. This conversion is necessary because most computer algebra softwares have built-in algorithms for effectively solving a system of ODEs [5,6]. The MOL was first proposed, discovered and presented by William Schiesser in [7]. Several other books have been published by him on the subject (see [5, 8–12]).

2 Derivation of the Governing PDE and Boundary Conditions

Let us represent the Generalized Morse interatomic potential

$$U_{\mathrm{GM}}(r) = \bar{A}e^{-\bar{\alpha}r} - \bar{B}e^{-\bar{\beta}r}, \tag{1}$$

where $\bar{A} > \bar{B} > 0$ and $\bar{\alpha} > \bar{\beta} > 0$ are constant parameters, in this form

$$U_{\mathrm{GM}}(r) = Ae^{-\bar{\alpha}(r-\bar{r})} - Be^{-\bar{\beta}(r-\bar{r})}, \tag{2}$$

where A and B are new amplitude parameters. Indeed,

$$A = \bar{A}e^{-\bar{\alpha}\bar{r}} \quad \text{and} \quad B = \bar{B}e^{-\bar{\beta}\bar{r}}. \tag{3}$$

Let us assume that the coordinate $\bar{r}$ corresponds to the minimum of $U_{\mathrm{GM}}(r)$ as presented in Figure 1,

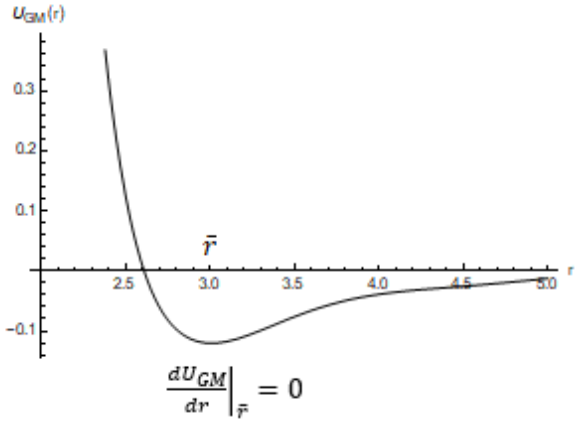

Figure 1: Potential energy curve of Generalized Morse potential for gold atom.

where $U'_{\mathrm{GM}}(r=\bar{r}) = \left.\dfrac{dU_{\mathrm{GM}}}{dr}\right|_{\bar{r}} = 0$. We differentiate Equation (2) with respect to r at the coordinate $r = \bar{r}$

$$\left.\frac{dU_{\mathrm{GM}}}{dr}\right|_{\bar{r}} = -\bar{\alpha}A + \bar{\beta}B = 0. \tag{4}$$

From Equation (3) and Equation (4), we obtain the coordinate of $\bar{r}$

$$\bar{r} = \frac{1}{\bar{\alpha}-\bar{\beta}} \ln\left(\frac{\bar{\alpha}\bar{A}}{\bar{\beta}\bar{B}}\right). \tag{5}$$

By substituting Equation (5) into Equation (3), the following expressions are derived:

$$\begin{aligned} A &= \bar{A}\exp\left[-\frac{\bar{\alpha}}{\bar{\alpha}-\bar{\beta}}\ln\left(\frac{\bar{\alpha}\bar{A}}{\bar{\beta}\bar{B}}\right)\right] = \bar{A}\left(\frac{\bar{\alpha}\bar{A}}{\bar{\beta}\bar{B}}\right)^{-\frac{\bar{\alpha}}{\bar{\alpha}-\bar{\beta}}}, \\ B &= \bar{B}\exp\left[-\frac{\bar{\beta}}{\bar{\alpha}-\bar{\beta}}\ln\left(\frac{\bar{\alpha}\bar{A}}{\bar{\beta}\bar{B}}\right)\right] = \bar{B}\left(\frac{\bar{\alpha}\bar{A}}{\bar{\beta}\bar{B}}\right)^{-\frac{\bar{\beta}}{\bar{\alpha}-\bar{\beta}}}. \end{aligned} \tag{6}$$

Let us consider a nonlinear chain of identical atoms (unit mass, m) in which the atoms at equilibrium are located at the distance, $\bar{r}$, with respect to each other, and assume that the linear longitudinal displacement of the k^{th} atom is $u_k = u_k(t)$, where $k = 1, 2, \ldots, N$ number of atoms in the chain. We only consider the interactions between the k^{th} and $(k+1)^{th}$ or $(k-1)^{th}$ and k^{th} atoms.

It is reasonable to apply the variational principles to simultaneously derive the governing PDE and possible boundary conditions. We write the kinetic energy of the continuum as

$$K = \int_0^l \frac{1}{2} m\dot{u}^2 dr, \tag{7}$$

where the stress $\dot{u} = \dfrac{\partial u(t,r)}{\partial t}$ and l is the length of the distributed chain. The potential energy of the continuum is

$$P = \int_0^l (Ae^{-\alpha u'} - Be^{-\beta u'}) dr, \tag{8}$$

where the strain $u' = \dfrac{\partial u(t,r)}{\partial r}$. It should be noted that

$$\alpha = \bar{\alpha}\bar{r},\ \beta = \bar{\beta}\bar{r}. \tag{9}$$

Hence, the Lagrangian of the continuum is $L = K - P = \displaystyle\int_0^l \Lambda dr$, where Λ is the Lagrangian density defined as

$$\Lambda = \Lambda(\dot{u}, u') = \frac{1}{2}m\dot{u}^2 - (Ae^{-\alpha u'} - Be^{-\beta u'}). \tag{10}$$

The explicit governing second-order PDE is

$$\frac{\partial^2 u}{\partial t^2} - \left[\bar{a}\exp\left(-\alpha\frac{\partial u}{\partial r}\right) - \bar{b}\exp\left(-\beta\frac{\partial u}{\partial r}\right)\right]\frac{\partial^2 u}{\partial r^2} = 0, \tag{11}$$

where

$$\bar{a} = \frac{\alpha^2 A}{m} = \frac{\bar{\alpha}^2 A}{m}\bar{r}^2,\ \bar{b} = \frac{\beta^2 B}{m} = \frac{\bar{\beta}^2 B}{m}\bar{r}^2.$$

There are four possible different combinations of the boundary conditions, and we select one of them, which is the fixed left end and the free right end

$$r = 0: \quad u(t, r = 0) = 0; \qquad r = l: \quad \left.\frac{\partial u}{\partial r}\right|_{r=l} = 0. \tag{12}$$

See Appendix A and B for the derivation.

3 Applying the Method of Lines to Obtain the Numerical Approximation of the Solution for the Governing PDE

The method of lines (MOL) is a semi-analytical approach that involves the conversion of a PDE to a coupled system of infinite ODEs [13, 14]. The PDE is converted to a coupled system of infinite ODEs by discretizing one of the spatial variables while using an analytical solution for the other spatial variable [14]. The coupled system of infinite ODEs can then be truncated to obtain a coupled system of finite ODEs.

For simplicity, we assume that $r = l$ becomes $r = 1$. In our case, we discretize the space variable r and use an analytical solution for the time variable t. The definitions for the first-order and second-order centered-difference formulas are

$$\left.\frac{\partial u_k(t)}{\partial r}\right|_{r=r_k} = \frac{1}{2\Delta r}[u_{k+1}(t) - u_{k-1}(t)], \tag{13}$$

$$\left.\frac{\partial^2 u_k(t)}{\partial r^2}\right|_{r=r_k} = \frac{1}{\Delta r^2}[u_{k-1}(t) - 2u_k(t) + u_{k+1}(t)], \tag{14}$$

where Δr is the spacing between the discretized lines, and $k = 1, 2, \ldots, N-1$. Finally, we write $\dfrac{\partial^2 u(t,r)}{\partial t^2} = \dfrac{d^2 u_k(t)}{dt^2}$. These definitions are introduced into Equation (11) and Equation (12) to obtain the coupled system of infinite second-order ODEs and new boundary conditions (See Appendix C).

We have partially discretised the space variable, r, of the function, $u(t,r)$, into a coupled system of infinite ODEs whose unknown solutions are $u_1(t), u_2(t), u_3(t), \ldots, u_{N-1}(t)$,

and we also converted the boundary conditions into initial conditions. It should be noted that $u_0(t) = 0, u_N(t) = u_{N-1}(t)$ and $k = 1, 2, \ldots, N-1$. The infinitely coupled system is truncated into a coupled system of finite ODEs, where $N = 60, 75, 150$. We select the initial conditions as $u_k(0) = A \sin \dfrac{\pi k}{2N}$, where A is the amplitude of the wave solution and $u_k'(0) = 0$ for $k = 1, 2, \ldots, N-1$. The value of the amplitude determines how the nonlinear terms in the continuum manifest themselves. We consider the initial conditions, corresponding to the boundary conditions, at the first mode of vibration of the linearized wave equation. The initial conditions for $A = 1.75$ are illustrated in Figure 2.

During the numerical simulations of the truncated system of ODEs, it was found that $A \in (0.0, 1.75]$. We did not consider negative values of the amplitude, A, because the negative values make the continuum oscillate in the opposite direction. The value of the amplitude to be used depends on the number of the truncated coupled system of finite ODEs to be numerically integrated. This is because the truncated coupled system of ODEs becomes a stiff system (with higher values of A) and the computer algebra software takes a lot of time in unsuccessfully integrating the problem. The time integration of the numerical analysis for the coupled system of ODEs was carried out within the interval $t \in [0, 4\pi]$ seconds.

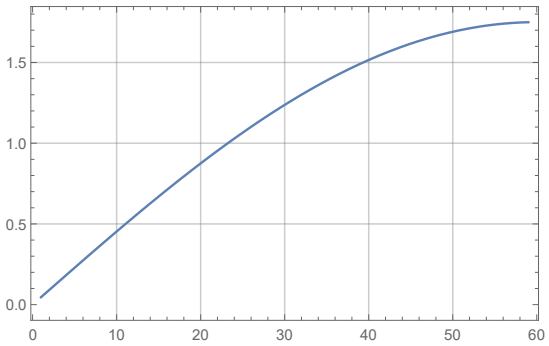

Figure 2: Graph of initial conditions, $u_k(0)$.

For convenience of numerical simulations, the parameters $\bar{a}, \bar{b}, \alpha$, and β were further scaled to the new parameters

$$a = \frac{\bar{a}}{\bar{a} - \bar{b}} \Delta r^{-2}, \quad b = \frac{\bar{b}}{\bar{a} - \bar{b}} \Delta r^{-2}, \quad \breve{\alpha} = \frac{\alpha}{20 \bar{r} \Delta r}, \quad \breve{\beta} = \frac{\beta}{20 \bar{r} \Delta r}.$$

We also defined the parameter values $m = 197, A = 0.058, B = 0.174$, and $\bar{r} = 3.006174$, where we choose the molar mass of the gold atom as the unit mass. It should be noted that $\bar{\alpha}, \bar{\beta}, \bar{A}$ and $\bar{B}$ have been calculated in [15, 16].

3.1 Numerical analysis of truncated coupled ODEs

The numerical simulations for a grid of 60 points using the amplitude value $A = 1.75$ is shown in Figure 3. Then, bearing in mind that the higher the number of lines, the more accurate the approximation, we consider the Equation (26) for higher grids, i.e., $N = 75, 150$ points, respectively. However, for higher number of lines, $N > 150$, the numerically approximated solution of the governing PDE significantly deteriorates. The

NDSolve framework of Wolfram Mathematica®, student edition, version 12.0.0.0 was used to numerically solve the truncated coupled system of ODEs. We also invoked the "Adams" sub-method (for computational time efficiency) with no specified "AccuracyGoal" or "PrecisionGoal" values defined. The amplitude for all the numerical simulation in Figure 3(a) to (d) was 1.75 and time interval $t \in [0, 4\pi]$ seconds. In nonlinear acoustics, the trough of the wave solutions in continuum mechanics is skewed and triangle-like. This was the case in Figure 3(d), which was also observed from Figure 3(b). In Figure 3(a), we see that the approximate solution for $u_1(t)$, is substantially deteriorated. This was due to the high value of the amplitude, A, used for the numerical simulation. Figure 3(c) displays how nonlinear terms in the continuum are manifested.

See Figure 4(a) to (d) for the numerical simulations of an amplitude value 1.0 and the number of grids having 75 points. Figure 4(b) and (e) reveals the wave troughs are still triangle-like through the entire solution, although not as sharp as those in Figure 3(b) and (e). The value of the amplitude is reasonable but still high. A comparison between Figure 3(b) and Figure 4(b) implies that the higher the value of the amplitude, the more skewed the troughs become all through the wave solution. Surprisingly, Figure 4(a) presents a symmetric solution as compared to Figure 3(a). This means the number of lines chosen and the value of the amplitude used influence the reliability of the approximate solution of the governing PDE.

For the next solution, we use an amplitude value of 0.04 and show numerical simulation results for 150 grid points. The solution plots display perfect symmetric edges (from a pictorial perspective) all through the wave solution. The effect of high amplitude is clearly observed in the comparisons between Figure 3(b), Figure 4(b) and Figure 5(b). The contour plots for Figure 3(b), Figure 4(b) and Figure 5(b) are each distinct because different amplitude values were used and the number of lines was varied. The lines in the contour plots clearly detail the manifestation of the nonlinear terms and the suppression of the terms.

3.2 Analysis of the periodic motion of the wave solution

Now, we want to calculate the spectrum of a number of cosine and sine harmonics using the Fourier coefficients for the right end of the continuum. We do this by taking into consideration the solution, $u_{149}(t)$, interpolate the solution, find the zeros of the solution using the LogPlot function of the absolute value for the interpolated function (in Wolfram Mathematica®), then we plot one period of the solution and integrate the plotted function from 0 to 2π in order to obtain the desired coefficients. Although the Fourier series are well-known and used in longitudinal oscillations in crystals, vibrating mechanical systems or in describing physical processes in which events recur in a regular pattern [17, 18], we apply the knowledge to understand the manifestation of nonlinear terms in the continuum of atoms.

Numerical simulations yielded the following harmonics for an amplitude value of 0.04:

$$\begin{array}{ll} c_0 = 2.674036 \times 10^{-4}, & \\ c_1 = -3.985559 \times 10^{-4}, & s_1 = 3.9736 \times 10^{-2}, \\ c_2 = 1.318224 \times 10^{-4}, & s_2 = 2.296953 \times 10^{-6}, \\ c_3 = 9.509503 \times 10^{-7}, & s_3 = -8.771975 \times 10^{-5}, \\ c_4 = -1.256332 \times 10^{-6}, & s_4 = 7.783809 \times 10^{-8}, \\ c_5 = -1.06498 \times 10^{-6}, & s_5 = 1.434977 \times 10^{-5}. \end{array} \tag{15}$$

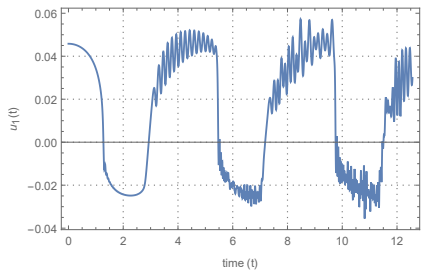

(a)

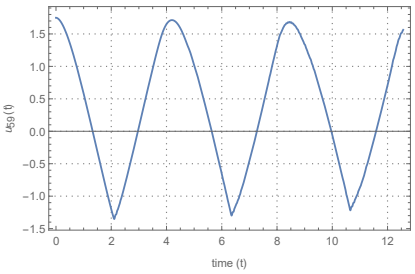

(b)

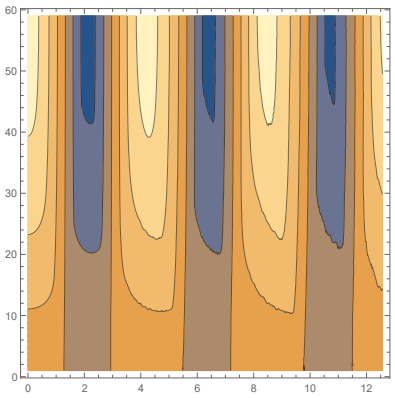

(c)

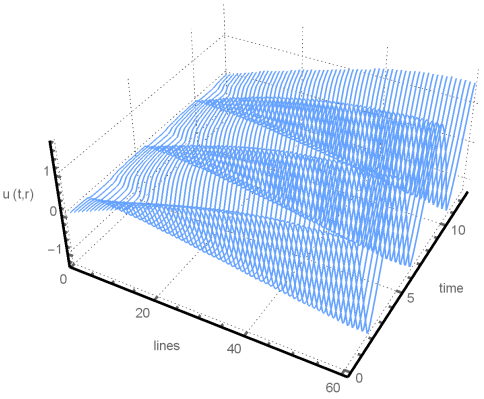

(d)

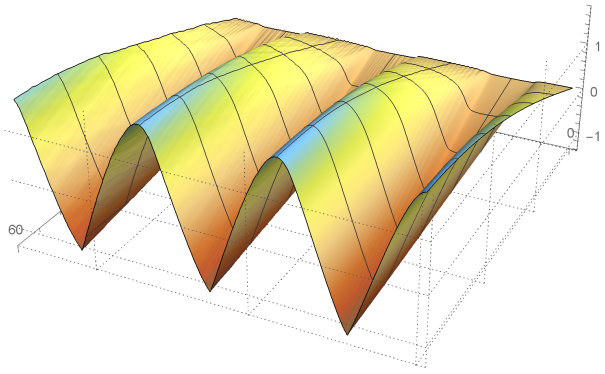

(e)

Figure 3: (a) First solution plot, $u_1(t)$, of the truncated coupled ODEs for $N = 60$ points; (b) Last solution plot, $u_{59}(t)$, of the truncated coupled ODEs for $N = 60$ points; (c) Contour plot of the truncated coupled ODEs for $N = 60$ points; (d) Parametric plot of the truncated coupled ODEs for $N = 60$ points; (e) Surface plot of the truncated coupled ODEs for $N = 60$ points.

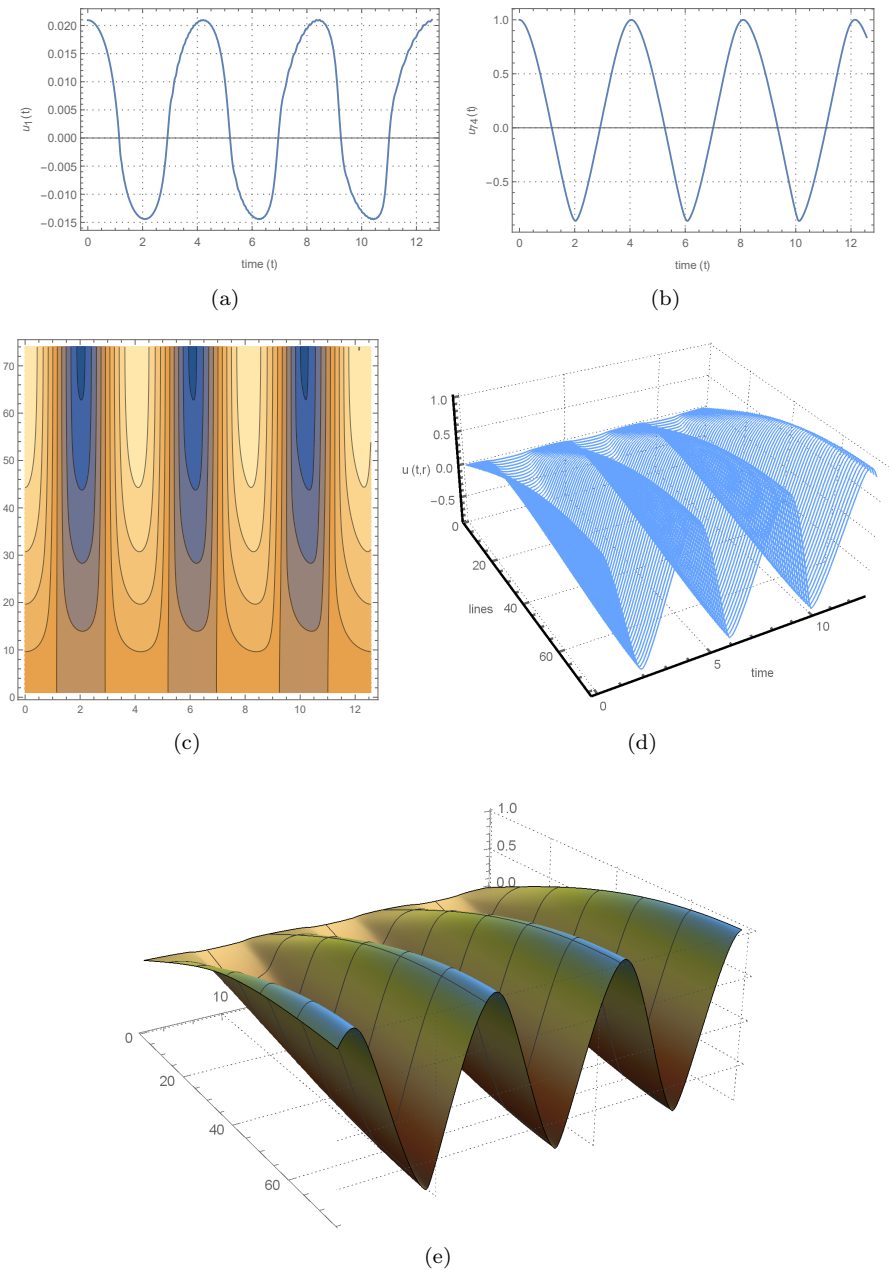

(a) (b) (c) (d) (e)

Figure 4: (a) First solution plot, $u_1(t)$, of the truncated coupled ODEs for $N = 75$ points; (b) Last solution plot, $u_{74}(t)$, of the truncated coupled ODEs for $N = 75$ points; (c) Contour plot of the truncated coupled ODEs for $N = 75$ points; (d) Parametric plot of the truncated coupled ODEs for $N = 75$ points; (e) Surface plot of the truncated coupled ODEs for $N = 75$ points.

Numerical simulations for an amplitude value of 0.25 yielded the following harmonics:

$$\begin{aligned} c_0 &= 9.945892 \times 10^{-3}, \\ c_1 &= -1.4423 \times 10^{-2}, & s_1 &= 2.41632 \times 10^{-1}, \\ c_2 &= 4.65619 \times 10^{-3}, & s_2 &= 5.031898 \times 10^{-4}, \\ c_3 &= 8.796602 \times 10^{-5}, & s_3 &= -2.461517 \times 10^{-3}, \\ c_4 &= -2.389894 \times 10^{-4}, & s_4 &= 1.930631 \times 10^{-5}, \\ c_5 &= -5.048646 \times 10^{-5}, & s_5 &= 2.905531 \times 10^{-4}. \end{aligned} \tag{16}$$

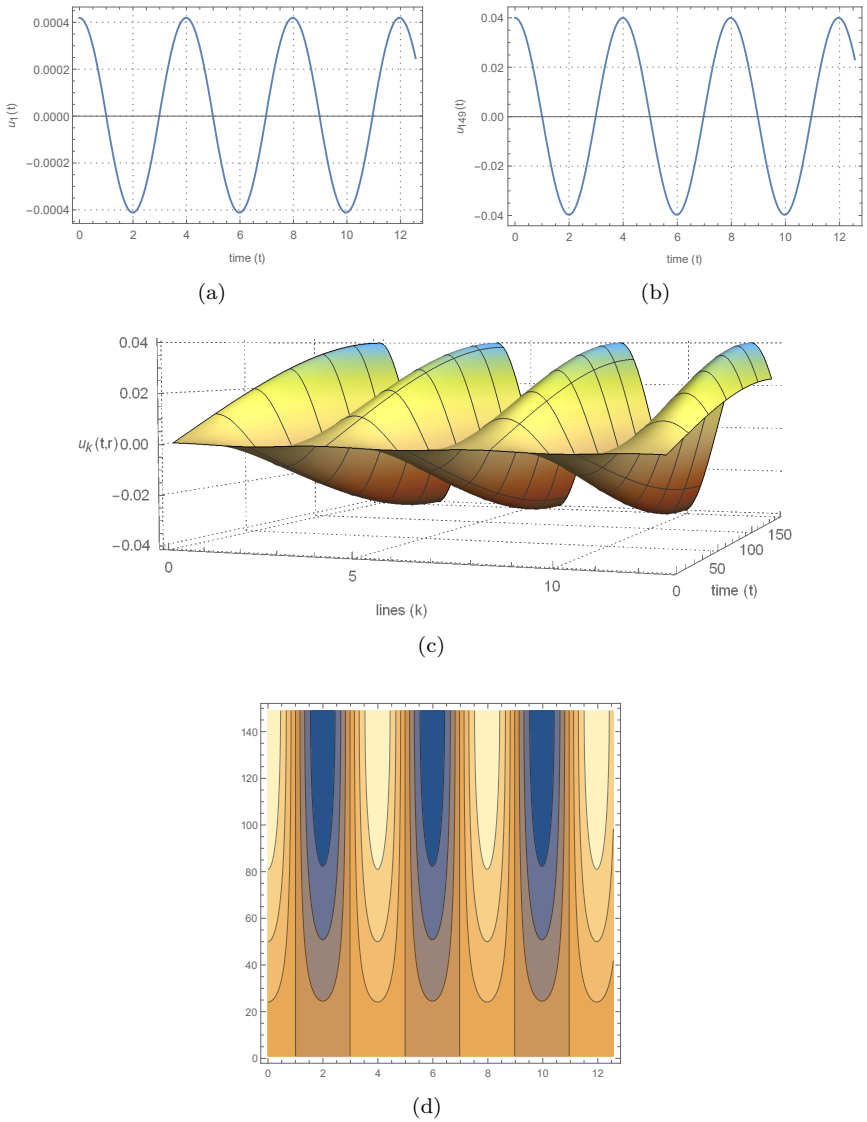

Figure 5: (a) First solution plot, $u_1(t)$, of the truncated coupled ODEs for $N = 150$ points; (b) Last solution plot, $u_{149}(t)$, of the truncated coupled ODEs for $N = 150$ points; (c) Contour plot of the truncated coupled ODEs for $N = 150$ points; (d) Surface plot of the truncated coupled ODEs for $N = 150$ points.

Numerical simulations for an amplitude value of 1.0 yielded the following harmonics:

$$\begin{aligned} &c_0 = 1.37004 \times 10^{-1}, \\ &c_1 = -1.81718 \times 10^{-1}, \quad && s_1 = 8.61703 \times 10^{-1}, \\ &c_2 = 4.5512 \times 10^{-2}, && s_2 = 2.3806 \times 10^{-2}, \\ &c_3 = 1.0145 \times 10^{-2}, && s_3 = -3.7237 \times 10^{-2}, \\ &c_4 = -1.0638 \times 10^{-2}, && s_4 = -4.446461 \times 10^{-3}, \\ &c_5 = -3.749745 \times 10^{-3}, && s_5 = 8.400466 \times 10^{-3}. \end{aligned} \tag{17}$$

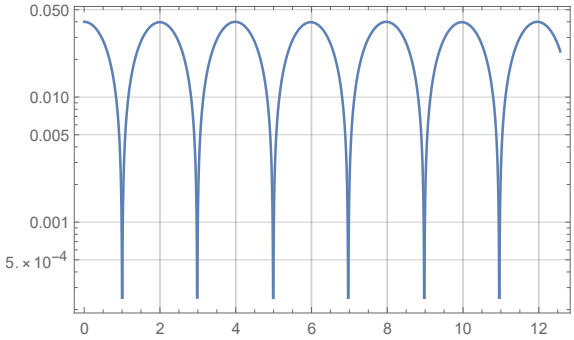

Figure 6: Zeros of interpolated function for $u_{149}(t)$ solution.

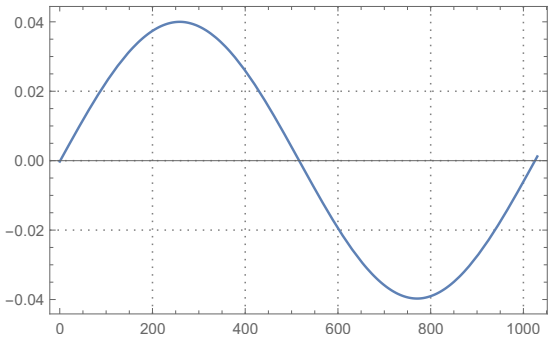

Figure 7: Plot of one period.

The numeric values in the respective harmonics for the respective amplitude show that the sine and cosine harmonics increase as the value of the amplitude is increased. This is therefore a substantial (and more reliable) measure of how nonlinear interactions in the continuum of gold atoms manifest. Although the simulation plots for amplitude values 0.25 and 0.04 will appear to be perfectly smooth, the calculation of the Fourier coefficients helps us to understand (by numerical computations) how the nonlinear terms are changing.

4 Discussion and Summary

A continuum describing an attachment of infinite atoms was theoretically investigated. The nonlinear interactions in the nanochain were described by the Generalized Morse potential energy function. A governing second-order PDE was derived using Hamilton's principle and the corresponding boundary conditions were also formulated. The MOL was employed to obtain approximate solutions of the continuum because of the PDE's complexity. The contour plots indicate how the nonlinear terms in the continuum are manifested or suppressed.

This study can be used as an example to understand the fast building of slender nanostructures/nanochain or one-dimensional lattices. This can be done by taking into consideration the dynamics which includes fast growing amplitudes and the manifestation

of nonlinear growth of nonlinear effects due to the large amplitudes of vibration as well as manifestation of nonlinear quadratic terms in the potential function.

It was generally observed that the waves motion towards the right end of the continuum became more skewed for increasing values of A. The formation of the sharp corners in longitudinal displacement (see Figures 3(b) and 4(b)) means the formation of discontinuity in the radial strain (which is equal to the derivative of displacement with respect to longitudinal coordinate). The strain discontinuity forms the stress discontinuity (Hooke's law). In continuous structures, the stresses must change continuously: "stress × area = applied force", but "action = reaction" due to Newton's third law. This means, at fast growth and oscillations, the long nanochains demonstrate the tendency for disruption. We can interpret this to be one of fundamental properties of asymmetry of the interatomic potentials, not only for the Morse potential investigated in this study.

Acknowledgments

The authors wish to thank Tshwane University of Technology for the postgraduate bursary support of Mr Surulere. The authors also acknowledge support from the Department of Higher Education and Training, South Africa.

A Derivation of explicit governing equation for the continuum

We introduce the functional of action

$$I = \int_0^t L d\tau = \int_0^t \int_0^l \Lambda dr d\tau, \tag{18}$$

and the variation of the functional of action

$$\delta I = \int_0^t \delta L d\tau = \int_0^t \int_0^l \delta\Lambda dr d\tau. \tag{19}$$

We know that

$$\delta\Lambda(\dot{u}, u') = \frac{\partial\Lambda}{\partial\dot{u}}\delta\dot{u}(t,r) + \frac{\partial\Lambda}{\partial u'}\delta u'(t,r). \tag{20}$$

Now, we can write

$$\delta\Lambda(\dot{u}, u') = \frac{\partial}{\partial t}\left[\frac{\partial\Lambda}{\partial\dot{u}}\delta u(t,r)\right] - \frac{\partial}{\partial t}\left(\frac{\partial\Lambda}{\partial\dot{u}}\right)\delta u(t,r) + \frac{\partial}{\partial r}\left[\frac{\partial\Lambda}{\partial u'}\delta u(t,r)\right] - \frac{\partial}{\partial r}\left(\frac{\partial\Lambda}{\partial u'}\right)\delta u(t,r). \tag{21}$$

Hamilton's principle at the stationary point is applied, i.e., $\delta I = 0$ while bearing in mind that $\delta u(t,r) = 0$ at the limits of integration, $\tau \in [0,t]$

$$\delta I = \int_0^t \left[\frac{\partial\Lambda}{\partial u'}\delta u(t,r)\right]_0^l d\tau - \int_0^t \int_0^l \left[\frac{\partial}{\partial t}\left(\frac{\partial\Lambda}{\partial\dot{u}}\right) + \frac{\partial}{\partial r}\left(\frac{\partial\Lambda}{\partial u'}\right)\right]\delta u(t,r) dr d\tau = 0. \tag{22}$$

Since $\delta u(t,r)$ is arbitrary, the fundamental lemma of calculus of variations requires that $\delta I = 0$ if and only if

$$\frac{\partial}{\partial t}\left(\frac{\partial\Lambda}{\partial\dot{u}}\right) + \frac{\partial}{\partial r}\left(\frac{\partial\Lambda}{\partial u'}\right) = 0, \quad \left[\frac{\partial\Lambda}{\partial u'}\delta u(t,r)\right]_{r=0}^{r=l} = 0.$$

The Euler-Lagrange equation presented in terms of the Lagrangian density (i.e., an implicit form of the Euler-Lagrange equation) is

$$\frac{\partial}{\partial t}\left(\frac{\partial \Lambda}{\partial \dot{u}}\right)+\frac{\partial}{\partial r}\left(\frac{\partial \Lambda}{\partial u'}\right)=0,$$

and possible boundary conditions for the continuum are

$$\begin{aligned} r=0: \qquad & [\delta u(t,r)]_{r=0}=0 \quad \text{or} \quad \left[\frac{\partial \Lambda}{\partial u'}\right]_{r=0}=0, \\ r=l: \qquad & [\delta u(t,r)]_{r=l}=0 \quad \text{or} \quad \left[\frac{\partial \Lambda}{\partial u'}\right]_{r=l}=0. \end{aligned} \tag{23}$$

We recall Equation (10) to obtain the expressions

$$\begin{aligned} \frac{\partial}{\partial r}\left(\frac{\partial \Lambda}{\partial u'}\right) =& \frac{\partial}{\partial r}\left[-\alpha A\exp(-\alpha u')+\beta B\exp(-\beta u')\right] \\ =& \left[\alpha^2 A\exp\left(-\alpha\frac{\partial u}{\partial r}\right)-\beta^2 B\exp\left(-\beta\frac{\partial u}{\partial r}\right)\right]\frac{\partial^2 u}{\partial r^2}, \\ \frac{\partial}{\partial t}\left(\frac{\partial \Lambda}{\partial \dot{u}}\right) =& \frac{\partial}{\partial t}(m\ddot{u})=m\frac{\partial^2 u}{\partial t^2}. \end{aligned} \tag{24}$$

B Derivation of boundary conditions

Before writing the explicit boundary conditions, let us remark that

$$\frac{\partial \Lambda}{\partial u'}=-\alpha A\exp(-\alpha u')+\beta B\exp(-\beta u'),$$

but from Equation (4), $\bar{\alpha}A=\bar{\beta}B$ and hence, $\alpha A=\beta B$. This means that $\dfrac{\partial \Lambda}{\partial u'}=0$ if and only if $\dfrac{\partial u}{\partial r}=0$. The explicit boundary conditions are then obtained from Equation (23)

$$\begin{aligned} r=0: \qquad & u(t,r=0)=0 \quad \text{or} \quad \left.\frac{\partial u}{\partial r}\right|_{r=0}=0, \\ r=l: \qquad & u(t,r=l)=0 \quad \text{or} \quad \left.\frac{\partial u}{\partial r}\right|_{r=l}=0. \end{aligned} \tag{25}$$

C Formulation of coupled system of infinite ODEs

Introducing definitions (13) and (14) into Equation (11) and Equation (12), we will obtain the coupled system of infinite second-order ODEs

$$\begin{aligned} \frac{d^2 u_k(t)}{dt^2}-&\left\{\bar{a}\exp\left(-\frac{\alpha}{2\Delta r}[u_{k+1}(t)-u_{k-1}(t)]\right)-\bar{b}\exp\left(-\frac{\beta}{2\Delta r}[u_{k+1}(t)-u_{k-1}(t)]\right)\right\} \\ &\times\frac{1}{(\Delta r)^2}[u_{k-1}(t)-2u_k(t)+u_{k+1}(t)]=0, \end{aligned} \tag{26}$$

and the new boundary conditions

$$r = 0: \quad u_k(0) = 0, \tag{27}$$

$$r = 1: \quad \frac{\partial u(t,r)}{\partial r}\Big|_{r=r_N} = 0. \tag{28}$$

At the boundary, $r = 1$, Equation (13) is replaced by the backward-difference (or implicit difference) method

$$\frac{\partial u_k(t)}{\partial r}\Big|_{r=r_k} = \frac{1}{2\Delta r}[u_k(t) - u_{k-1}(t)]. \tag{29}$$

Evaluating Equation (29) at $r = r_N$ and comparing with Equation (26) give the expression $\dfrac{1}{2\Delta r}[u_N(t) - u_{N-1}(t)] = 0$. This simply means $u_N(t) = u_{N-1}(t)$.

References

[1] B. I. Iliya. *Vibrational Mechanics: Nonlinear Dynamic Effects, General Approach, Applications*. World Scientific Publishing Co. Ptc. Ltd, 2000.

[2] M. Toda. Vibration of a chain with nonlinear interaction. *Journal of the Physical Society of Japan* **22** (2) (1967) 431–436.

[3] M. Toda. *Theory of Nonlinear Lattices*, Vol. 20. Springer Science & Business Media, 2012.

[4] P. M. Morse. Diatomic molecules according to the wave mechanics. II. Vibrational levels. *Physical Review* **34** (1) (1929) 57.

[5] W. E. Schiesser and G. W. Griffiths. *A Compendium of Partial Differential Equation Models: Method of Lines Analysis With Matlab*. Cambridge University Press, 2009.

[6] F. Shakeri and M. Dehghan. The method of lines for solution of the one-dimensional wave equation subject to an integral conservation condition. *Computers & Mathematics with Applications* **56** (9) (2008) 2175–2188.

[7] W. Schiesser. *The Numerical Method of Lines: Integration of Partial Differential Equations*. Academic Press, 1991.

[8] W. E. Schiesser. *Partial Differential Equation Analysis in Biomedical Engineering: Case Studies with Matlab*. Cambridge University Press, 2012.

[9] W. E. Schiesser. *Method of Lines Pde Analysis in Biomedical Science and Engineering*. John Wiley & Sons, 2016.

[10] W. E. Schiesser. *Method of Lines Analysis of Turing Models*. World Scientific, 2017.

[11] W. Schiesser. Method of lines solution of the Korteweg-de Vries equation. *Computers & Mathematics with Applications* **28** (10-12) (1994) 147–154.

[12] P. Saucez, W. Schiesser and A. V. Wouwer. Upwinding in the method of lines. *Mathematics and Computers in Simulation* **56** (2) (2001) 171–185.

[13] J. N. M. Bidie. An error analysis of the numerical method of lines, Master's thesis. Tshwane University of Technology, South Africa, 2011.

[14] M. N. Sadiku and C. Obiozor. A simple introduction to the method of lines. *International journal of electrical engineering education* **37** (3) (2000) 282–296.

[15] S. Surulere, M. Shatalov, A. Mkolesia, T. Malange and A. Adeniji. The integral-differential and integral approach for the exact solution of the hybrid functional forms for Morse potential. *IAENG International Journal of Applied Mathematics* **50** (2) (2020) 242–250.

[16] S. A. Surulere, M. Y. Shatalov, A. C. Mkolesia and I. Fedotov. Vibrations in a growing nonlinear chain. *Discontinuity, Nonlinearity and Complexity*, in press (2020).

[17] A. Jeffrey. *Advanced Engineering Mathematics*. Elsevier, 2001.

[18] D. G. Duffy. Advanced Engineering Mathematics with Matlab. CRC Press, 2016.